

Correlations of density and current fluctuations in single-file motion of hard spheres and in driven lattice gas with nearest-neighbor interaction

Sören Schweers,^{1,*} Gunter M. Schütz,^{2,†} and Philipp Maass^{1,‡}

¹*Universität Osnabrück, Institute for Physics, BarbarasträÙe 7, D-49076 Osnabrück, Germany*

²*IAS 2, Forschungszentrum Jülich, 52425 Jülich, Germany.*

(Dated: February 20, 2025)

We analyze correlations between density fluctuations and between current fluctuations in a one-dimensional driven lattice gas with repulsive nearest-neighbor interaction and in single-file Brownian motion of hard spheres dragged across a cosine potential with constant force. By extensive kinetic Monte Carlo and Brownian dynamics simulations we show that density and current correlation functions in nonequilibrium steady states follow the scaling behavior of the Kardar-Parisi-Zhang (KPZ) universality class. In a coordinate frame comoving with the collective particle velocity, the current correlation function decays as $\sim -t^{-4/3}$ with time t . Density fluctuations spread superdiffusively as $\sim t^{2/3}$ at long times and their spatio-temporal behavior is well described by the KPZ scaling function. In the absence of the cosine potential, the correlation functions in the system of dragged hard spheres show scaling behavior according to the Edwards-Wilkinson universality class. In the coordinate frame comoving with the mean particle velocity, they behave as in equilibrium, with current correlations decaying as $\sim -t^{-3/2}$ and density fluctuations spreading diffusively as $\sim t^{1/2}$.

I. INTRODUCTION

In single-file motion, particles cannot overtake each other and accordingly keep their ordering [1–4]. This type of motion occurs, for example, in confined colloidal systems [5–12], zeolites [13–15], nanotubes [16–20], membrane channels [21–31], molecular motors along filaments [32–35], and ribosome translation [36–43]. Particle density fluctuations and current fluctuations in these systems are intertwined [44, 45] and reflect phenomena like superdiffusive spreading of density fluctuations [46, 47] and excess mass flow through interfaces [48]. They are key for understanding subtle effects in nonequilibrium dynamics, as, for example, recently found long-range anticorrelations in the stochastic motion of domain walls separating phases in driven diffusive systems [49].

In equilibrium, autocorrelations of density and current fluctuations take a Gaussian shape, while they are usually non-Gaussian in nonequilibrium steady states (NESS) and can be described by the scaling function of the Kardar-Parisi-Zhang (KPZ) universality class [45, 50–53]. KPZ scaling is seen in many models, such as height-height correlations of interface growth under ballistic deposition [45, 50, 51], spin-spin correlations of the Heisenberg chain [54], correlations of locally conserved quantities (mass, momentum, energy) in one-dimensional Newtonian fluids [52], as well as density correlations in driven lattice gases [44, 55, 56].

For diffusive systems, studies of density and current correlations have so far focused on the symmetric and totally asymmetric simple exclusion processes (SEP and TASEP) [57, 58]. In these models, particles jump between nearest sites of a one-dimensional lattice, where

each lattice site can be occupied by at most one particle, corresponding to an exclusion interaction. In the SEP the rates for jumps to the left and right are equal, while in the TASEP jumps are allowed in one direction only.

In the SEP with mean particle density $\bar{\rho}$, correlation functions

$$C_{\rho\rho}(x, t) = \langle \delta\rho(x, t)\delta\rho(0, 0) \rangle = \langle \rho(x, t)\rho(0, 0) \rangle - \bar{\rho}^2 \quad (1)$$

between fluctuations $\delta\rho(x, t) = \rho(x, t) - \bar{\rho}$ of the local particle density $\rho(x, t)$ spread diffusively in the equilibrium state, i.e. they broaden with the square root of time. They obey the scaling law

$$C_{\rho\rho}(x, t) \sim \frac{\kappa}{\sqrt{2D_{\rho\rho}t}} G\left(\frac{x}{\sqrt{2D_{\rho\rho}t}}\right) \quad (2)$$

of the Edwards-Wilkinson (EW) universality class [59], where $\kappa = \int dx C_{\rho\rho}(x, t)$, $D_{\rho\rho}$ is a $\bar{\rho}$ -dependent diffusion coefficient, and $G(\cdot)$ is the standard Gaussian, $G(u) = \exp(-u^2/2)/\sqrt{2\pi}$ [45]. Time correlations

$$C_{JJ}(t) = \langle J(x, t)J(x, 0) \rangle \quad (3)$$

between currents $J(x, t)$ at the same position (site) x decay as [45]

$$C_{JJ}(t) \sim -A_{\text{eq}} t^{-3/2}, \quad t \rightarrow \infty, \quad (4)$$

where A_{eq} is a constant with approximate value

$$A_{\text{eq}} \simeq \frac{1}{8} D_{\rho\rho}^{1/2} \kappa \int dx |x| G(x) = \frac{\kappa}{4\sqrt{2\pi}} D_{\rho\rho}^{1/2}. \quad (5)$$

For the TASEP, density and current correlations show scaling behavior in a nonequilibrium steady state (NESS), when they are recorded in a comoving frame with collective velocity [58]

$$v = v(\bar{\rho}) = \frac{d\bar{J}(\bar{\rho})}{d\bar{\rho}}, \quad (6)$$

* sschweers@uos.de

† gschuetz04@yahoo.com

‡ maass@uos.de

where $\bar{J}(\bar{\rho})$ is the stationary current at mean particle density $\bar{\rho}$. Density fluctuations spread superdiffusively in this frame, broadening in time as $\sim t^{2/3}$. The $C_{\rho\rho}(x, t)$ obey the scaling form

$$C_{\rho\rho}(x, t) \sim \frac{\kappa}{(\Gamma_{\rho\rho}t)^{2/3}} F_{\text{KPZ}}\left(\frac{x-vt}{(\Gamma_{\rho\rho}t)^{2/3}}\right), \quad (7)$$

where $\kappa = \int dx C_{\rho\rho}(x, t)$, $\Gamma_{\rho\rho}$ is a $\bar{\rho}$ -dependent rate of superdiffusive spreading, and $F_{\text{KPZ}}(\cdot)$ is the KPZ scaling function. Its exact form was derived by Prähofer and Spohn [60]. The rate of spreading is proportional to the absolute value of the second derivative $\bar{J}''(\bar{\rho})$ [45, 61], $\Gamma_{\rho\rho} \propto |\bar{J}''(\bar{\rho})|$.

The superdiffusive scaling of density fluctuations in NESS is reflected in long-range anticorrelations between currents across an interface moving with velocity $v(\bar{\rho})$ [48]. Considering the respective local currents $J_{\text{cf}}(x, t) = J(x+vt, t) - v\rho(x+vt, t)$ in the comoving frame with average $\bar{J}_{\text{cf}} = \bar{J} - v\bar{\rho}$, the time correlations of their fluctuations

$$\begin{aligned} C_{JJ}^{\text{cf}}(t) &= \langle \delta J_{\text{cf}}(x, t) \delta J_{\text{cf}}(x, 0) \rangle \\ &= \langle J_{\text{cf}}(x, t) J_{\text{cf}}(x, 0) \rangle - \bar{J}_{\text{cf}}^2 \end{aligned} \quad (8)$$

decay as [45]

$$C_{JJ}^{\text{cf}}(t) \sim -At^{-4/3}, \quad t \rightarrow \infty, \quad (9)$$

where A is a constant, which for zero collective velocity $v(\bar{\rho}) = 0$ is approximately

$$A \simeq \frac{1}{9} \Gamma_{\rho\rho}^{2/3} \kappa \int dx |x| F_{\text{KPZ}}(x). \quad (10)$$

Equations (1)-(10) describe long-time asymptotic behavior and should hold true irrespective of microscopic details for driven diffusive systems of particles with short-range interactions. Here we test this for a lattice gas with repulsive nearest-neighbor interactions and for a system with continuous-space dynamics, given by overdamped Brownian dynamics of hard spheres. In particular, we evaluate whether correlations between current fluctuations decay with the expected power laws and whether the long-time behavior becomes visible beyond microscopic times scales without extended transients. For the continuous-space system, we present a method to cope with the problem of computing local fluctuations in a comoving frame.

II. BROWNIAN MOTION OF HARD SPHERES AND LATTICE GAS WITH NEAREST-NEIGHBOR INTERACTION

Overdamped Brownian motion of hard spheres in a periodic potential and particle hopping in a lattice with repulsive nearest-neighbor interactions are illustrated in Fig. 1 together with current-density relations $\bar{J}(\bar{\rho})$ in these systems. In the following, we specify the dynamics in the two models.

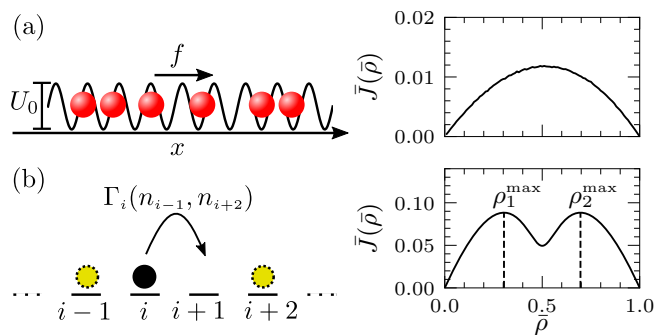


FIG. 1. (a) Left: Overdamped Brownian motion of hard spheres across a sinusoidal potential [Eq. (11)] with barriers U_0 under a constant drag force f . Right: Bulk current-density relation $\bar{J}(\bar{\rho})$ for parameters $U_0/k_B T = 6$, $f\lambda/k_B T = 1$, and $\sigma = 0.8\lambda$. (b) Left: Particle hopping in a lattice with repulsive nearest-neighbor interactions, where rates $\Gamma(n_{i-1}, n_{i+2})$ for a particle jump from a site i to a vacant site $i+1$ depend on the occupation numbers n_{i-1} and n_{i+2} of neighboring sites $i-1$ and $i+2$. Right: Bulk current-density relation $\bar{J}(\bar{\rho})$ for Glauber rates [Eq. (15)] with parameters $V/k_B T = 2V_c/k_B T = 4 \ln 3$. It has two maxima at ρ_1^{max} and ρ_2^{max} .

A. Brownian motion of hard spheres

Figure 1(a) illustrates overdamped Brownian motion of N hard spheres with diameter σ that are driven by a constant drag force f across a sinusoidal potential

$$U(x) = \frac{U_0}{2} \cos\left(\frac{2\pi x}{\lambda}\right). \quad (11)$$

Here, λ is the wavelength of the potential and U_0 the barrier between potential wells. This model was introduced as Brownian ASEP (BASEP), since it can be viewed as extension of the ASEP to continuous-space space dynamics [62].

The BASEP constitutes a basis for understanding various intriguing phenomena occurring in Brownian single-file transport through periodic potentials. This includes particle-size dependent current-density relations and non-equilibrium phase transition diagrams with up to five phases [62–64], faster uphill transitions in kinetics of local barrier passing [65], effective barrier enhancements in flow-driven system caused by hydrodynamic interactions [66, 67], ultrafast defect propagation and emergence of solitary cluster waves in dense systems [68–71], as well as phase synchronisation of collective dynamics and fractional Shapiro steps in particle currents under time-periodic driving [72].

The particle motion in the BASEP is described by the Langevin equations

$$\frac{dx_i}{dt} = \mu \left(f - \frac{\partial U(x_i)}{\partial x} \right) + \sqrt{2D} \xi_i(t), \quad (12)$$

where x_i , $i = 1, \dots, N$, are the particle positions, μ is the particle mobility, $D = k_B T \mu$ is the diffusion constant, and

$k_B T$ thermal energy. The $\xi_i(t)$ are uncorrelated stationary Gaussian processes with zero mean and correlation function $\langle \xi_i(t) \xi_j(t') \rangle = \delta_{ij} \delta(t - t')$. Periodic boundary conditions are applied for a system of length L . The mean particle density is $\bar{\rho} = N/L$.

The hard-sphere interaction implies the constraints

$$|x_i - x_j| \geq \sigma. \quad (13)$$

Their consideration requires special care in simulations [73–75]. Here we use the recently developed Brownian cluster dynamics algorithm [76, 77].

The bulk current-density relation $\bar{J}(\bar{\rho})$ for the BASEP was studied in [62, 63] and is shown in Fig. 1(a) for $\sigma = 0.8\lambda$, $U_0 = 6k_B T$ and $f = k_B T/\lambda$.

For vanishing periodic potential ($U_0 = 0$), the current-density relation is

$$\bar{J} = \mu f \bar{\rho}. \quad (14)$$

In this special case of a linear current-density relation, the EW rather than the KPZ universality class applies: density and local current autocorrelations behave according to Eqs. (2) and (4) as in an equilibrium system, if one determines the correlation functions in a frame comoving with the mean particle velocity $v(\bar{\rho}) = d\bar{J}(\bar{\rho})/d\bar{\rho} = \mu f$. The non-applicability of KPZ scaling is reflected in $\Gamma_{\rho\rho} \propto |\bar{J}''(\bar{\rho})|$ becoming zero for a linear current-density relation.

Physically, the absence of KPZ scaling for driven hard-spheres in a flat potential $U_0 = 0$ can be understood from the fact that dynamics in such system are equivalent to that of point particles [3, 78]. This follows after a simultaneous transformation $x_i \rightarrow x'_i = x_i - i\sigma$ of the particle coordinates and of the system size, $L \rightarrow L' = L - N\sigma$. For point particles, collective properties are the same as for independent particles [79]. Accordingly, for such properties the hard-sphere interaction becomes irrelevant in flat potentials. Let us note that this holds true also for dynamics of hard spheres in the presence of an external periodic potential with wavelength λ , if the particle diameter is an integer multiple of λ [63].

We use λ , $k_B T$, and $\lambda^2/D = \lambda^2/k_B T\mu$ as length, energy and time unit in the modeling; unit of force thus is $k_B T/\lambda$. If $U_0 = 0$, σ replaces λ as length unit.

B. Lattice gas with nearest-neighbor interaction

Figure 1(b) illustrates particle hopping in a one-dimensional driven lattice gas with repulsive nearest-neighbor interaction V [80–83]. The particles jump unidirectionally to unoccupied neighboring sites to their right. The lattice has L sites $i = 1, \dots, L$ and periodic boundary condition are applied. A lattice site can be occupied by at most one particle. Microstates of the system are given by the sets $\{n_i\}$ of occupation numbers, where $n_i = 1$ if site i is occupied by a particle and zero

otherwise. The rate of a particle jump from site i to a vacant site ($i + 1$) is given by the Glauber form

$$\Gamma_i(n_{i-1}, n_{i+2}) = \frac{\nu}{\exp(\beta V[n_{i+2} - n_{i-1}]) + 1}, \quad (15)$$

where ν is an attempt frequency and $\beta = 1/k_B T$.

We use the first-reaction time algorithm [84, 85] to simulate hopping dynamics by kinetic Monte-Carlo simulations.

The current-density relation is [80, 82, 83]

$$\bar{J}(\bar{\rho}) = \nu \left[\left(\bar{\rho} - C^{(1)} \right)^2 \frac{2g - 1}{2\bar{\rho}(1 - \bar{\rho})} + \left(\bar{\rho} - C^{(1)} \right) (1 - g) \right] \quad (16)$$

where

$$C^{(1)} = \frac{1}{2[1 - \exp(-\beta V)]} \left[2\bar{\rho}(1 - \exp(-\beta V)) - 1 + \sqrt{1 - 4\bar{\rho}(1 - \bar{\rho})[1 - \exp(-\beta V)]} \right] \quad (17)$$

and

$$g = \frac{1}{\exp(\beta V) + 1}. \quad (18)$$

$C^{(1)}$ in Eq. (17) is the correlation $\langle n_i n_{i+1} \rangle_{\text{eq}}$ in an equilibrium state of a lattice gas with nearest-neighbor interaction V . If the interaction exceeds a critical value V_c , $\beta V_c = 2 \ln 3$, the current-density relation has two degenerate maxima, $\bar{J}(\rho_1^{\text{max}}) = \bar{J}(\rho_2^{\text{max}})$ with $\rho_1^{\text{max}} \neq \rho_2^{\text{max}}$. For $V = 2V_c$, which we use in the following, these maxima are at $\rho_1^{\text{max}} = (1 - [3 - \sqrt{8e^{\beta V}/(e^{\beta V} - 1)}]^{1/2})/2 \cong 0.304$ and $\rho_2^{\text{max}} = 1 - \rho_1^{\text{max}} \cong 0.696$ [82, 83].

We use the lattice constant a and the inverse attempt frequency ν^{-1} as length and time unit in the modeling of the driven lattice gas.

III. SCALING OF DENSITY CORRELATIONS AND LONG-RANGE ANTICORRELATIONS BETWEEN CURRENT FLUCTUATIONS

In the analysis of the hard sphere system, we divide the system into L/σ boxes of size σ , which can accommodate at most one particle. To each box i at time t , we assign an occupation number $n_i(t) \in \{0, 1\}$, i.e. we obtain a description as in a lattice gas with lattice constant σ . This way we can calculate correlation functions as for a lattice gas.

To determine $C_{\rho\rho}(x, t)$, we first generate time series of the occupation numbers $n_i(k\Delta t)$, $k = 1, \dots, M$, with time step $\Delta t = \nu^{-1}$ in the lattice gas and time step $\Delta t = \sigma^2/D$ in the hard-sphere system. In equilibrium and nonequilibrium steady states, we then correlate fluctuations $\delta n_i(k'\Delta t) = n_i(k'\Delta t) - \bar{n}$ and $\delta n_{i+j}(k'\Delta t + k\Delta t)$ at distance $x = ja$ and time lag $t = k\Delta t$.

For calculating current correlations in the comoving frame, we determine link currents $j_{i,i+1}(t) = [n(i \rightarrow i +$

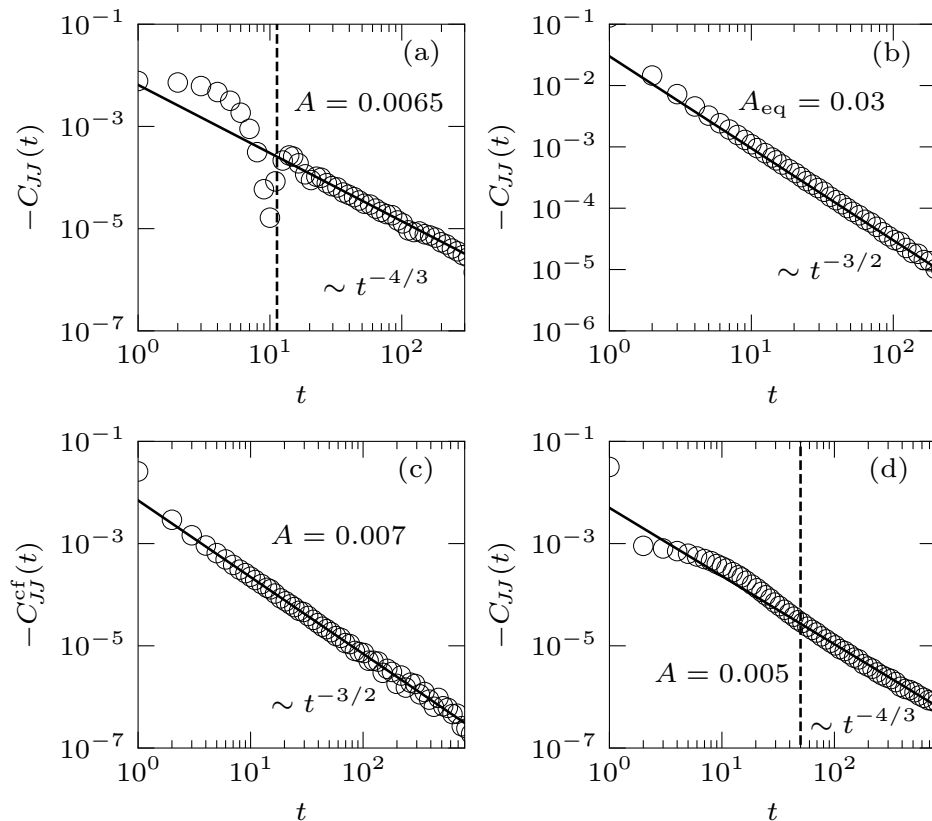


FIG. 2. Correlations between current fluctuations for (a) the TASEP with repulsive next-neighbor interactions $V = 2V_c$ at density $\bar{\rho} = \rho_1^{\max}$ and (b)-(d) Brownian single-file motion of hard spheres with particle density $\bar{\rho} = 1/2$. Data for hard-sphere systems are shown for three different situations: (b) an equilibrium state in a flat potential ($U_0 = 0$), (c) a nonequilibrium steady state of dragged spheres ($f = 1$) in a flat potential ($U_0 = 0$), and (d) a nonequilibrium steady state of dragged spheres ($f = 1$) in a sinusoidal potential ($U_0 = 6$). Solid lines are least-square fits of the power laws with exponents $-3/2$ [Eq. (4)] and $-4/3$ [Eq. (9)] to the asymptotic regime at long times (last 30 data points were used). The amplitude factors A_{eq} and A are the parameters obtained from the fits. Dashed vertical lines in (a) and (d) indicate estimates of times for the onset of the power law decay (see text). Data points were obtained by averaging the correlation functions in small bins with equal spacing on the logarithmic time axis.

1) $-n(i+1 \rightarrow i)]/\Delta t$ between all pairs of neighboring lattice sites $i, i+1$ at discrete times $t = l\Delta t, l = 1, 2, \dots$, where $n(i \rightarrow i+1)$ and $n(i+1 \rightarrow i)$ are the numbers of particles moving from site i to $(i+1)$ and vice versa in the time interval $]t, t+\Delta t]$. The link currents $j_{i,i+1}^{\text{cf}}(t)$ at time t in the frame comoving with the collective velocity v [Eq. (6)] are $j_{i,i+1}^{\text{cf}}(t) = j_{k,k+1}(t) - n_{k+1}(t+\Delta t)v$, where $k = j + vt$. For $v \neq 0$, we set $\Delta t = 1/|v|$ for the time step Δt , guaranteeing that vt is an integer. For $v = 0$, we use the same Δt as in the calculation of $C_{\rho\rho}(x, t)$.

A. Long-range anticorrelations between local current fluctuations

Figure 2 shows correlation functions of local current fluctuations for (a) the driven lattice gas at $\bar{\rho} = \rho_1^{\max}$ [see Fig. 1(b)], and (b)-(d) the hard sphere system at $\bar{\rho} = 1/2$. In Fig. 2(b) the results are for the equilibrium system in the absence of the periodic potential, i.e. for $f = 0$ and

$U_0 = 0$. In Figs. 2(c) and (d) the results are for the nonequilibrium system ($f = 1$), where in (c) $U_0 = 0$, and in (d) $U_0 = 6$ and $\sigma = 0.8$. As the current fluctuations are anticorrelated, we plotted the negative of the correlation functions in the double-logarithmic representations. In Fig. 2(c), the collective velocity is $v = \mu f = 1$, and it is zero in Figs. 2(a),(b) and (d).

In all cases the current correlation functions show the expected power law decay at large times: $C_{JJ}(t) \sim t^{-4/3}$ in Figs. 2(a),(d), and a decay $\sim t^{-3/2}$ in Figs. 2(b),(c).

Amplitude factors A_{eq} and A of the power laws were obtained from a least-square fitting of Eqs. (4) and (9) to the long-time regimes of the simulated data, see the values given in Figs 2(a)-(d). For the situation considered in Fig. 2(a) and (b), we can compare these numbers with the predicted approximate values in Eqs. (5) and (10). To calculate A and A_{eq} from these equations, we used the values $\kappa, \Gamma_{\rho\rho}$ or $D_{\rho\rho}$ obtained from the analysis of the density autocorrelation functions in Sec. III B, see Figs. 3(a)-(b). The resulting $A \cong 0.0051$ and $A_{\text{eq}} \cong 0.067$

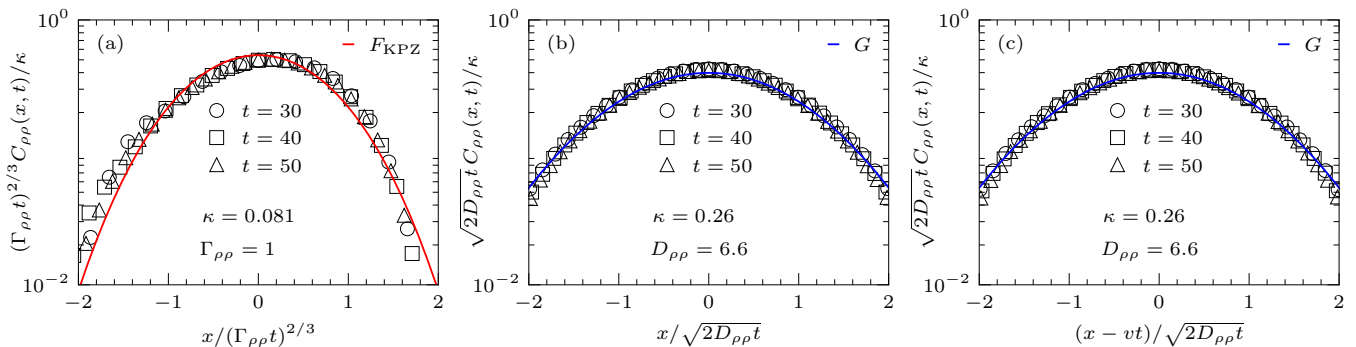


FIG. 3. Scaled correlation functions of particle density fluctuations for the same systems as in Figs. 2(a)-(c). The κ values were obtained by numerical integration of the unscaled correlation functions $C_{\rho\rho}(x, t)$. Parameters $\Gamma_{\rho\rho}$ and $D_{\rho\rho}$ were found by an optimal match of the normalized functions $F_{\text{KPZ}}(\cdot)$ and $G(\cdot)$ in Eqs. (7) and (2) to the scaled simulated data.

are of the order as the values given in Figs. 2(a) and (b).

In Figs. 2(b),(c) the data approach the power law decay $\sim t^{-3/2}$ from the beginning, while a different behavior is seen in Figs. 2(a),(d) at small microscopic time scales. The power law decay $\sim t^{-4/3}$ in Fig. 2(a) sets in for times larger than the inverse mean hopping rate of the particle. In Fig. 2(d), the onset time can be estimated by the time for the particles to pass their typical spacing $1/\bar{\rho} - \sigma$. With the mean particle velocity $\bar{J}/\bar{\rho}$, we get $t_{\times} \simeq (1 - \bar{\rho}\sigma)/\bar{J}$. Both estimated onset times are indicated by the vertical dashed lines in Figs. 2(a) and (d).

B. Scaling behavior of correlations between density fluctuations

While it is straightforward to determine density correlations in space and time by the numerical procedure described at the beginning of this section, a thorough analysis of their scaling behavior is extremely costly regarding computing time and data storage requirements [86]. We could not obtain $C_{\rho\rho}(x, t)$ over many orders of magnitudes in space and time, which would be necessary to check the theoretically predicted scaling properties based on the simulated data for $C_{\rho\rho}(x, t)$ alone. However, using the results from Sec. III A for the current correlations $C_{JJ}(t)$, we can perform an analysis with the assurance that scaling behavior is either according to Eq. (2) or Eq. (7).

Figures 3(a)-(c) show scaling plots of $C_{\rho\rho}(x, t)$ according to Eqs. (2) and (7) for the same systems as in Figs. 2(a)-(c). For the hard-spheres driven across the sinusoidal potential, we could not obtain data with sufficient numerical accuracy over a significant length scale covering several wavelengths λ .

The scaled data in Figs. 3(a)-(c) for three different times collapse onto common master curves. We determined the constant κ by numerical integration of $C_{\rho\rho}(x, t)$. For obtaining the value $\Gamma_{\rho\rho} = 1$ in Fig. 3(a) we fitted the parameter $\Gamma_{\rho\rho}$ by an optimal match of $(\Gamma_{\rho\rho} t)^{2/3} C_{\rho\rho}(x, t)/\kappa$ to the KPZ scaling function. For

$F_{\text{KPZ}}(\cdot)$, we used the tabulated data in [87]. Likewise, the value $D_{\rho\rho} = 6.6$ in Figs. 3(b),(c) was obtained by fitting the parameter $D_{\rho\rho}$ to give an optimal match with the standard Gaussian.

IV. SUMMARY AND CONCLUSIONS

We have tested the appearance of EW and KPZ scaling for correlations between density fluctuations and for related power law decays of correlations between local current fluctuations in single-file dynamics of a discrete and continuous-space systems. For the discrete system, we considered a driven lattice gas with repulsive nearest-neighbor interactions. For a representative system with continuous-space dynamics we studied Brownian motion of hard spheres in different situations: equilibrium dynamics in a flat potential as well as driven transport under a constant drag force in a flat and periodic potential with barriers of height six times the thermal energy.

Our simulation results are in agreement with theoretically predicted scaling behaviors: for the driven lattice gas and the hard spheres driven across the periodic potential, local current correlations are anticorrelated at long times and decay as $\sim t^{-4/3}$. Density correlations for the lattice gas spread superdiffusively as $\sim t^{2/3}$ and are described by the KPZ scaling function. For hard spheres in the periodic potential, a corresponding analysis of correlations between density fluctuations was unfortunately not feasible with our computational resources.

In the flat potential, the single-file dynamics of hard spheres showed scaling features according to the EW universality class for both the equilibrium and the driven system: correlations between local current fluctuations are anticorrelated and decay as $\sim t^{-3/2}$ at long times and correlations between density fluctuations spread diffusively and are described by the Gaussian scaling function. For the driven system, Gaussian scaling is present because the current-density relation is linear.

Long-range anticorrelated current fluctuations in driven single file transport are important for stochastic

dynamics of domain walls between coexisting nonequilibrium phases, which occur in open systems coupled to particle reservoirs [80, 88]. As shown recently [49], the power-law decay $\sim t^{-4/3}$ leads to a $t^{1/3}$ subdiffusive growth of the width of domain wall position fluctuations, if the domain walls separate coexisting extremal current phases. The collective velocity $v(\bar{\rho}) = d\bar{J}(\bar{\rho})/d\bar{\rho}$ is zero in both coexisting phases in that case because the densities of these phases are extrema of the bulk current-density relation $\bar{J}(\bar{\rho})$. Generically, for domain walls separating coexisting phases the width of wall position fluctuations grows diffusively as $t^{1/2}$ as long as $t^{1/2}/L \ll 1$ in a system of length L [89–92]. This scaling behavior corresponds to an effective random walk dynamics of the domain wall position. Indeed, this random walk property, which implies a Gaussian shape of the distribution of the domain wall position, has recently been proved rigorously [93] for some parameter manifolds in the ASEP. An intriguing open question is the distribution of the position in the case of the subdiffusive growth of the position fluctuations [49].

Mapping of particle positions in continuous-space sys-

tems to occupation numbers of small bins is a suitable method also for testing scaling behavior of density correlations in experiments. For the interpretation of experimental data, one can estimate $v(\bar{\rho}) = d\bar{J}(\bar{\rho})/d\bar{\rho}$ by measuring particle currents at densities around $\bar{\rho}$ and by taking a numerical derivative.

ACKNOWLEDGMENTS

This work has been funded by the Deutsche Forschungsgemeinschaft (DFG, Project No. 355031190), by FCT/Portugal through project UIDB/04459/2020 with DOI identifier 10-54499/UIDP/04459/2020, and through the grant 2022.09232.PTDC with DOI identifier 10.54499/2022.09232.PTDC. We sincerely thank A. Ryabov and the members of the DFG Research Unit FOR2692 for fruitful discussions. We acknowledge use of a high-performance computing cluster funded by the Deutsche Forschungsgemeinschaft (DFG, Project No. 456666331).

-
- [1] J. Kärger, Transport phenomena in nanoporous materials, *ChemPhysChem* **16**, 24 (2015).
- [2] K. Nygård, Colloidal diffusion in confined geometries, *Phys. Chem. Chem. Phys.* **19**, 23632 (2017).
- [3] A. Taloni, O. Flomenbom, R. Castañeda-Priego, and F. Marchesoni, Single file dynamics in soft materials, *Soft Matter* **13**, 1096 (2017).
- [4] B. C. Bukowski, F. J. Keil, P. I. Ravikovitch, G. Sastre, R. Q. Snurr, and M.-O. Coppens, Connecting theory and simulation with experiment for the study of diffusion in nanoporous solids, *Adsorption* **27**, 683 (2021).
- [5] Q.-H. Wei, C. Bechinger, and P. Leiderer, Single-file diffusion of colloids in one-dimensional channels, *Science* **287**, 625 (2000).
- [6] B. Cui, H. Diamant, and B. Lin, Screened hydrodynamic interaction in a narrow channel, *Phys. Rev. Lett.* **89**, 188302 (2002).
- [7] B. Lin, B. Cui, J.-H. Lee, and J. Yu, Hydrodynamic coupling in diffusion of quasi-one-dimensional brownian particles, *Europhys. Lett. (EPL)* **57**, 724 (2002).
- [8] C. Lutz, M. Kollmann, and C. Bechinger, Single-file diffusion of colloids in one-dimensional channels, *Phys. Rev. Lett.* **93**, 026001 (2004).
- [9] C. Lutz, M. Kollmann, P. Leiderer, and C. Bechinger, Diffusion of colloids in one-dimensional light channels, *J. Phys.: Condens. Mat.* **16**, S4075 (2004).
- [10] B. Lin, M. Meron, B. Cui, S. A. Rice, and H. Diamant, From random walk to single-file diffusion, *Phys. Rev. Lett.* **94**, 216001 (2005).
- [11] M. Köppl, P. Henseler, A. Erbe, P. Nielaba, and P. Leiderer, Layer reduction in driven 2D-colloidal systems through microchannels, *Phys. Rev. Lett.* **97**, 208302 (2006).
- [12] P. Henseler, A. Erbe, M. Köppl, P. Leiderer, and P. Nielaba, Density reduction and diffusion in driven two-dimensional colloidal systems through microchannels, *Phys. Rev. E* **81**, 041402 (2010).
- [13] K. Hahn, J. Kärger, and V. Kukla, Single-file diffusion observation, *Phys. Rev. Lett.* **76**, 2762 (1996).
- [14] K. Hahn and J. Kärger, Deviations from the normal time regime of single-file diffusion, *J. Phys. Chem. B* **102**, 5766 (1998).
- [15] C. Chmelik, J. Caro, D. Freude, J. Haase, R. Valiullin, and J. Kärger, Diffusive Spreading of Molecules in Nanoporous Materials, in *Diffusive Spreading in Nature, Technology and Society*, edited by A. Bunde, J. Caro, J. Kärger, and G. Vogl (Springer International Publishing, Cham, 2018) Chap. 10, pp. 171–202.
- [16] C.-Y. Cheng and C. R. Bowers, Observation of single-file diffusion in dipeptide nanotubes by continuous-flow hyperpolarized Xenon-129 NMR spectroscopy, *ChemPhysChem* **8**, 2077 (2007).
- [17] A. Das, S. Jayanthi, H. S. M. V. Deepak, K. V. Ramanathan, A. Kumar, C. Dasgupta, and A. K. Sood, Single-file diffusion of confined water inside SWNTs: An NMR study, *ACS Nano* **4**, 1687 (2010).
- [18] M. Dvoyashkin, H. Bhase, N. Mirnazari, S. Vasenkov, and C. R. Bowers, Single-file nanochannel persistence lengths from NMR, *Anal. Chem.* **86**, 2200 (2014).
- [19] W. Cao, L. Huang, M. Ma, L. Lu, and X. Lu, Water in narrow carbon nanotubes: Roughness promoted diffusion transition, *J. Phys. Chem. C* **122**, 19124 (2018).
- [20] S. Zeng, J. Chen, X. Wang, G. Zhou, L. Chen, and C. Dai, Selective transport through the ultrashort carbon nanotubes embedded in lipid bilayers, *J. Phys. Chem. C* **122**, 27681 (2018).
- [21] P. Graf, A. Nitzan, M. G. Kurnikova, and R. D. Coalson, A dynamic lattice monte carlo model of ion transport in inhomogeneous dielectric environments: Method and implementation, *J. Phys. Chem. B* **104**, 12324 (2000).

- [22] A. B. Mamonov, R. D. Coalson, A. Nitzan, and M. G. Kurnikova, The role of the dielectric barrier in narrow biological channels: A novel composite approach to modeling single-channel currents, *Biophys. J.* **84**, 3646 (2003).
- [23] P. Graf, M. G. Kurnikova, R. D. Coalson, and A. Nitzan, Comparison of dynamic lattice Monte Carlo simulations and the dielectric self-energy Poisson-Nernst-Planck continuum theory for model ion channels, *J. Phys. Chem. B* **108**, 2006 (2004).
- [24] W. R. Bauer and W. Nadler, Molecular transport through channels and pores: Effects of in-channel interactions and blocking, *Proc. Natl. Acad. Sci. U.S.A.* **103**, 11446 (2006).
- [25] M. Kahms, P. Lehrich, J. Hüve, N. Sanetra, and R. Peters, Binding site distribution of nuclear transport receptors and transport complexes in single nuclear pore complexes, *Traffic* **10**, 1228 (2009).
- [26] S. Y. Yang, J.-A. Yang, E.-S. Kim, G. Jeon, E. J. Oh, K. Y. Choi, S. K. Hahn, and J. K. Kim, Single-file diffusion of protein drugs through cylindrical nanochannels, *ACS Nano* **4**, 3817 (2010).
- [27] M. Einax, G. C. Solomon, W. Dieterich, and A. Nitzan, Unidirectional hopping transport of interacting particles on a finite chain, *J. Chem. Phys.* **133**, 054102 (2010).
- [28] P. H. Nelson, A permeation theory for single-file ion channels: One- and two-step models, *J. Chem. Phys.* **134**, 165102 (2011).
- [29] B. Luan and R. Zhou, Single-file protein translocations through Graphene-MoS₂ heterostructure nanopores, *J. Phys. Chem. Lett.* **9**, 3409 (2018).
- [30] M. Zhao, W. Wu, and B. Su, pH-controlled drug release by diffusion through silica nanochannel membranes, *ACS Appl. Mater. Interfaces* **10**, 33986 (2018).
- [31] J. Kärger, D. M. Ruthven, and R. Valiullin, Diffusion in nanopores: inspecting the grounds, *Adsorption* **27**, 267 (2021).
- [32] R. Lipowsky, J. Beeg, R. Dimova, S. Klumpp, and M. J. Müller, Cooperative behavior of molecular motors: Cargo transport and traffic phenomena, *Physica E* **42**, 649 (2010), Proceedings of the international conference Frontiers of Quantum and Mesoscopic Thermodynamics FQMT '08.
- [33] D. Chowdhury, Stochastic mechano-chemical kinetics of molecular motors: A multidisciplinary enterprise from a physicist's perspective, *Phys. Rep.* **529**, 1 (2013).
- [34] A. B. Kolomeisky, *Motor Proteins and Molecular Motors* (CRC Press, Boca Raton, 2015).
- [35] A. Jindal, A. B. Kolomeisky, and A. K. Gupta, The role of dynamic defects in transport of interacting molecular motors, *J. Stat. Mech. Theor. Exp.* , 043206 (2020).
- [36] C. T. MacDonald, J. H. Gibbs, and A. C. Pipkin, Kinetics of biopolymerization on nucleic acid templates, *Biopolymers* **6**, 1 (1968).
- [37] G. M. Schütz, The Heisenberg chain as a dynamical model for protein synthesis - some theoretical and experimental results, *Int. J. Mod. Phys. B* **11**, 197 (1997).
- [38] L. Ciandrini, I. Stansfield, and M. C. Romano, Role of the particle's stepping cycle in an asymmetric exclusion process: A model of mRNA translation, *Phys. Rev. E* **81**, 051904 (2010).
- [39] S. Klumpp and T. Hwa, Stochasticity and traffic jams in the transcription of ribosomal RNA: Intriguing role of termination and antitermination, *Proc. Natl. Acad. Sci. USA* **105**, 18159 (2008).
- [40] R. K. P. Zia, J. J. Dong, and B. Schmittmann, Modeling translation in protein synthesis with TASEP: A tutorial and recent developments, *J. Stat. Phys.* **144**, 405 (2011).
- [41] D. D. Erdmann-Pham, K. Dao Duc, and Y. S. Song, The key parameters that govern translation efficiency, *Cell Syst.* **10**, 183 (2020).
- [42] J. Keisers and J. Krug, Exclusion model of mRNA translation with collision-induced ribosome drop-off, *J. Phys. A Math. Theor.* **56**, 385601 (2023).
- [43] D. Chowdhury, A. Schadschneider, and K. Nishinari, Physics of collective transport and traffic phenomena in biology: Progress in 20 years., *Phys. Life Rev.* **51**, 409 (2024).
- [44] M. Prähofer and H. Spohn, Current fluctuations for the totally asymmetric simple exclusion process, in *In and Out of Equilibrium: Probability with a Physics Flavor*, edited by V. Sidoravicius (Birkhäuser Boston, Boston, MA, 2002) pp. 185–204.
- [45] P. L. Ferrari and H. Spohn, On time correlations for KPZ growth in one dimension, *SIGMA* **12**, 074 (2016).
- [46] H. van Beijeren, R. Kutner, and H. Spohn, Excess noise for driven diffusive systems, *Phys. Rev. Lett.* **54**, 2026 (1985).
- [47] V. A. Popkov, A. Schadschneider, J. Schmidt, and G. M. Schütz, Fibonacci family of dynamical universality classes, *Proc. Natl. Acad. Sci. U.S.A.* **112**, 12645 (2015).
- [48] H. van Beijeren, Fluctuations in the motions of mass and of patterns in one-dimensional driven diffusive systems, *J. Stat. Phys.* **63**, 47 (1991).
- [49] S. Schweers, D. F. Locher, G. M. Schütz, and P. Maass, Weak pinning and long-range anticorrelated motion of phase boundaries in driven diffusive systems, *Phys. Rev. Lett.* **132**, 167101 (2024).
- [50] M. Kardar, G. Parisi, and Y.-C. Zhang, Dynamic scaling of growing interfaces, *Phys. Rev. Lett.* **56**, 889 (1986).
- [51] H. Spohn, The Kardar-Parisi-Zhang equation: a statistical physics perspective, in *Stochastic Processes and Random Matrices: Lecture Notes of the Les Houches Summer School: Volume 104, July 2015* (Oxford University Press, 2017).
- [52] H. Spohn, The 1 + 1 dimensional Kardar-Parisi-Zhang equation: more surprises, *J. Stat. Mech: Theory Exp.* **2020**, 044001 (2020).
- [53] J. Quastel and S. Sarkar, Convergence of exclusion processes and KPZ equation to the KPZ fixed point, *J. Am. Math. Soc.* **36**, 251 (2023).
- [54] J. D. Nardis, S. Gopalakrishnan, and R. Vasseur, Nonlinear fluctuating hydrodynamics for Kardar-Parisi-Zhang scaling in isotropic spin chains, *Phys. Rev. Lett.* **131**, 197102 (2022).
- [55] Priyanka and K. Jain, Critical dynamics of the jamming transition in one-dimensional nonequilibrium lattice-gas models., *Phys. Rev. E* **93**, 042104 (2015).
- [56] J. de Gier, A. Schadschneider, J. Schmidt, and G. M. Schütz, Kardar-Parisi-Zhang universality of the Nagel-Schreckenberg model, *Phys. Rev. E* **100**, 052111 (2019).
- [57] B. Derrida, An exactly solvable non-equilibrium system: The asymmetric simple exclusion process, *Phys. Rep.* **301**, 65 (1998).
- [58] G. M. Schütz, Exactly solvable models for many-body systems far from equilibrium, in *Phase Transitions and Critical Phenomena*, Vol. 19, edited by C. Domb and J. L. Lebowitz (Academic Press, 2001) pp. 1–251.
- [59] J. Krug, Origins of scale invariance in growth processes,

- Adv. Phys.* **46**, 139 (1997).
- [60] M. Prähofer and H. Spohn, Exact scaling functions for one-dimensional stationary KPZ growth, *J. Stat. Phys.* **115**, 255 (2004).
- [61] J. Krug, P. Meakin, and T. Halpin-Healy, Amplitude universality for driven interfaces and directed polymers in random media, *Phys. Rev. A* **45**, 638 (1992).
- [62] D. Lips, A. Ryabov, and P. Maass, Brownian asymmetric simple exclusion process, *Phys. Rev. Lett.* **121**, 160601 (2018).
- [63] D. Lips, A. Ryabov, and P. Maass, Single-file transport in periodic potentials: The Brownian asymmetric simple exclusion process, *Phys. Rev. E* **100**, 052121 (2019).
- [64] D. Lips, A. Ryabov, and P. Maass, Nonequilibrium transport and phase transitions in driven diffusion of interacting particles, *Z. Naturforsch. A* **75**, 449 (2020).
- [65] A. Ryabov, D. Lips, and P. Maass, Counterintuitive short uphill transitions in single-file diffusion, *J. Phys. Chem. C* **123**, 5714 (2019).
- [66] E. Cereceda-López, D. Lips, A. Ortiz-Ambriz, A. Ryabov, P. Maass, and P. Tierno, Hydrodynamic interactions can induce jamming in flow-driven systems, *Phys. Rev. Lett.* **127**, 214501 (2021).
- [67] D. Lips, E. Cereceda-López, A. Ortiz-Ambriz, P. Tierno, A. Ryabov, and P. Maass, Hydrodynamic interactions hinder transport of flow-driven colloidal particles, *Soft Matter* **18**, 8983 (2022).
- [68] A. P. Antonov, D. Voráč, A. Ryabov, and P. Maass, Collective excitations in jammed states: ultrafast defect propagation and finite-size scaling, *New J. Phys.* **24**, 093020 (2022).
- [69] A. P. Antonov, A. Ryabov, and P. Maass, Solitons in overdamped Brownian dynamics, *Phys. Rev. Lett.* **129**, 080601 (2022).
- [70] E. Cereceda-López, A. P. Antonov, A. Ryabov, P. Maass, and P. Tierno, Overcrowding induces fast colloidal solitons in a slowly rotating potential landscape, *Nat. Commun.* **14**, 6448 (2023).
- [71] A. P. Antonov, A. Ryabov, and P. Maass, Solitary cluster waves in periodic potentials: Formation, propagation, and soliton-mediated particle transport, *Chaos, Solitons & Fractals* **185**, 115079 (2024).
- [72] S. Mishra, A. Ryabov, and P. Maass, Phase locking and fractional Shapiro steps in collective dynamics of microparticles, to appear in *Phys. Rev. Lett.* (2025).
- [73] P. Strating, Brownian dynamics simulation of a hard-sphere suspension, *Phys. Rev. E* **59**, 2175 (1999).
- [74] A. Scala, T. Voigtmann, and C. De Michele, Event-driven Brownian dynamics for hard spheres, *J. Chem. Phys.* **126**, 134109 (2007).
- [75] A. Scala, Event-driven Langevin simulations of hard spheres, *Phys. Rev. E* **86**, 026709 (2012).
- [76] A. P. Antonov, S. Schweers, A. Ryabov, and P. Maass, Brownian dynamics simulations of hard rods in external fields and with contact interactions, *Phys. Rev. E* **106**, 054606 (2022).
- [77] A. P. Antonov, S. Schweers, A. Ryabov, and P. Maass, Fast Brownian cluster dynamics, *Comput. Phys. Commun.* **309**, 109474 (2025).
- [78] L. Tonks, The complete equation of state of one, two and three-dimensional gases of hard elastic spheres, *Phys. Rev.* **50**, 955 (1936).
- [79] A. Ryabov and P. Chvosta, Single-file diffusion of externally driven particles, *Phys. Rev. E* **83**, 020106 (2011).
- [80] V. Popkov and G. M. Schütz, Steady-state selection in driven diffusive systems with open boundaries, *Europhys. Lett.* **48**, 257 (1999).
- [81] T. Antal and G. M. Schütz, Asymmetric exclusion process with next-nearest-neighbor interaction: Some comments on traffic flow and a nonequilibrium reentrance transition, *Phys. Rev. E* **62**, 83 (2000).
- [82] M. Dierl, P. Maass, and M. Einax, Classical driven transport in open systems with particle interactions and general couplings to reservoirs, *Phys. Rev. Lett.* **108**, 060603 (2012).
- [83] M. Dierl, M. Einax, and P. Maass, One-dimensional transport of interacting particles: Currents, density profiles, phase diagrams, and symmetries, *Phys. Rev. E* **87**, 062126 (2013).
- [84] D. T. Gillespie, Monte Carlo simulation of random walks with residence time dependent transition probability rates, *J. Comput. Phys.* **28**, 395 (1978).
- [85] V. Holubec, P. Chvosta, M. Einax, and P. Maass, Attempt time Monte Carlo: An alternative for simulation of stochastic jump processes with time-dependent transition rates, *Europhys. Lett.* **93**, 40003 (2011).
- [86] For generating one data set, 1000 CPU cores of a HPC cluster with AMD EPYC 7742 CPUs were used for one day.
- [87] M. Prähofer and H. Spohn, Data for the function $g(u)$, whose second derivative $g''(u)$ gives $F_{\text{KPZ}}(u) = g''(u)/4$ (2002), <http://www-m5.ma.tum.de/KPZ/>.
- [88] J. Krug, Boundary-induced phase transitions in driven diffusive systems, *Phys. Rev. Lett.* **67**, 1882 (1991).
- [89] G. Schütz and E. Domany, Phase transitions in an exactly soluble one-dimensional exclusion process, *J. Stat. Phys.* **72**, 277 (1993).
- [90] B. Derrida, S. A. Janowsky, J. L. Lebowitz, and E. R. Speer, Exact solution of the totally asymmetric simple exclusion process: Shock profiles, *J. Stat. Phys.* **73**, 813 (1993).
- [91] A. B. Kolomeisky, G. M. Schütz, E. B. Kolomeisky, and J. P. Straley, Phase diagram of one-dimensional driven lattice gases with open boundaries, *J. Phys. A: Math. Gen.* **31**, 6911 (1998).
- [92] M. L. Dudzinski and G. M. Schütz, Relaxation spectrum of the asymmetric exclusion process with open boundaries, *J. Phys. A: Math. Gen.* **33**, 8351 (2000).
- [93] G. M. Schütz, A reverse duality for the ASEP with open boundaries, *J. Phys. A Math. Theor.* **56**, 274001 (2023).